1 Physics benefits

1.1 Introduction

The proposed trigger processor will perform the following tasks:

- find all hit clusters in the SMT
- determine the cluster centroid (by forming pulseheight-weighted averages) and the total pulseheight of every cluster;
- provide L3 with the cluster and pulseheight information
- find tracks in the roads determined from track candidates found by the L1 CFT trigger
- determine the track parameters (transverse momentum, impact parameter) and send them to the L2 global processor
- find the z-positions of the primary vertices of the $\bar{p}p$ interaction(s) during the beam crossing, using the clusters found in the 90°stereo strips, and send the z-values and the corresponding track multiplicity to L3.

The additional information, namely p_T with a better resolution than would be available at L2 without STT, the impact parameter, and the z-position of the vertices, provide powerful handles that can be used in the trigger decision to reduce background trigger rate and/or increase signal efficiency. In this section, we describe some of the studies that we have done to assess and quantify the benefits that the STT could bring to our physics program.

1.2 Trigger simulation

1.2.1 Data Samples

A number of studies were done to assess the physics benefits and understand the potential performance of the STT [1, 2, 3, 4, 5, 6, 7, 8, 9]. For this purpose Monte Carlo events were generated with various generators (ISAJET, PYTHIA, COMPHEP) and then underwent full detector simulation using UPG_GEANT. After that, they were converted to the standard run II trigger simulation ntuple[10]. Three types of data samples were used in these studies:

- single track events, with and without additional minimum bias events overlayed;
- signal events, with and without additional minimum bias events overlayed;
- background events.

All of the samples were generated with the mean primary vertex position at (0.,0.,0.). The z co-ordinate of the primary vertex was smeared with a Gaussian of width 25 cm. The effect of lateral smearing of the primary vertex position due to the finite beam size was found to have a small effect on the conclusions about the efficiency vs. background rejection power of the trigger [2] (see also subsection 1.4.

A summary of the signal events used for these studies is given in Table 1. More details about these samples can be found in the respective DØ notes [1, 3, 4, 5, 6, 7, 8, 9].

The QCD background sample was the standard run II trigger studies sample[11]. The sample consists of dijet events generated in six hard-scatter E_T bins. For each E_T bin, samples were created with 1, 3, 5, or 7 additional minimum bias interactions. Trigger rates and pass fractions used in this study were obtained by a weighted sum of the results from each of the 24 samples. The weight for a given sample was the ISAJET cross section times the probability of seeing the number of interactions corresponding to the generated file. The results for +0, +2, +4, +6 and +8 interactions (where no events were generated) were found by interpolating the results from the generated files. The weighted sum is performed automatically within the run II trigger package[11].

Table 1: Signal events

reaction	generator	add'l min. bias	number of events
$t\bar{t} \to$ *all jets*	ISAJET	0	2126
$t\bar{t} \to$ *all jets*	ISAJET	3	500
$t\bar{t} \to \mu +$ *jets*	ISAJET	0	1175
$Z \to b\bar{b}$	ISAJET	0	9979
$Z \to b\bar{b}$	ISAJET	2	995
$Z \to b\bar{b}$	ISAJET	5	995
$p\overline{p} \to WH^0 \to q\bar{q}b\overline{b}$	Pythia V5.7	0	1700
$t \to W \to e\nu$	COMPHEP	0	20000
$t \to W \to \mu\nu$	COMPHEP	0	20000
$t \to W \to jj$	COMPHEP	0	5000
$Q\bar{Q} \to \mu\mu X$	NLO	0	45000
$Q\bar{Q} \to e^+e^-X$	NLO	0	45000
$b \to J/\psi + X, J/\psi \to \mu^+\mu^-$	ISAJET	0	
$b \to J/\psi + X, J/\psi \to e^+e^-$	ISAJET	0	
direct $J/\psi + X$	ISAJET	0	9760
$B_d^o \to K_s^o + J/\psi$	ISAJET	0	
$B_s \to D_s^- + \mu^+ + \nu_\mu$	ISAJET	0	2275
$B_s \to D_s^- + 3\pi^\pm$	ISAJET	0	2323

1.2.2 Simulation of trigger performance

The trigger ntuple maker package is an attempt to simulate L1 and L2 trigger conditions for run 2. For every detector foreseen for run 2, that information is calculated from the raw GEANT data which will be available at the trigger level. Therefore it allows the study of the effects of additional trigger conditions beyond the standard trigger menu which does not use the SMT information. The track finding algorithm used in the trigger simulation code for the CFT at L1 is the algorithm foreseen for the actual trigger implementation in run 2 [12, 13, 14].

The track finding algorithm for the STTpp at L2 used in the code[15] is such that it could be implemented in the hardware that we anticipate using. It assumes that the L1 CFT trigger provides information about track candidates found at L1. The roads defined by the L1 CFT information are then extrapolated into the SMT and the hits within the road are used in the track fit. The equation used for the extrapolation is $\varphi(r) = \kappa r + \varphi_0$, where $\kappa = \frac{eB}{2p_T}$ is the curvature, $\varphi_0 = \varphi(r=0)$, and r is the distance from nominal beam line to the detector element. Using fiber tracker (CFT) and silicon (SMT) hits, the track parameters are then determined by a χ^2 minimization, fitting the hits to the equation $\varphi(r) = \frac{b}{r} + \kappa r + \phi_0$, where b is the impact parameter. This is a good approximation as long as the track length is small compared to the radius of the track helix. The equations can be linearized by expanding parameters about a central track

$$p_j = p_j^c + \sum_{i=1}^{n} \left(\frac{\partial p_j}{\partial \varphi_i}\right)_c (\varphi_i - \varphi_i^c).$$

This way, the parameter fits are reduced to products and sums. Derivatives can be calculated ahead of time and stored in a LUT. In the studies done so far, the central track was taken as the center of the CFT road projection into the SMT, and the SMT hits considered in the fit were those closest to the center of the CFT road. It turned out that this choice of hits to be used in the fit was not always the correct one, in particular for tracks with large impact parameter. To remedy for the resulting inefficiency, the STT tracks with reduced $\chi^2 > 4$ were refitted after having dropped the SMT hit giving the largest contribution to the χ^2 [16]. Only those tracks associated with hits in at least 3 layers of the SMT and with reduced $\chi^2 \leq 4$ were considered "good" STT tracks. All of the performance and physics benefit studies reported here used these track quality cuts, and the signal efficiencies quoted include the inefficiency due to these cuts. It should be noted that it is conceivable that the tracking algorithms that will be used in the final implementation may well be more sophisticated than the one used in the simulation, thus possibly improving the efficiency beyond the values found in our studies.

1.2.3 Performance Studies

p_T resolution:
Using single track events containg a μ or e with $|\eta| \leq 1.0$ and $1.5 \leq p_T \leq 15$ GeV, the CFT momentum was computed three ways:

- "CFT(a)": use CFT fibers in inner and outer layer only; (this is the information about L1 CFT track candidates broadcast to L2)
- "CFT(b)": use p_t^{min} and p_t^{max}, the momentum limits from the CFT track equation, i.e. $\frac{1}{p_t} = \frac{1}{2}(\frac{1}{p_t^{min}} + \frac{1}{p_t^{max}})$ (This is the momentum as determined and used for a decision at L1.)
- "STT": use both SMT and CFT(a) information in fit

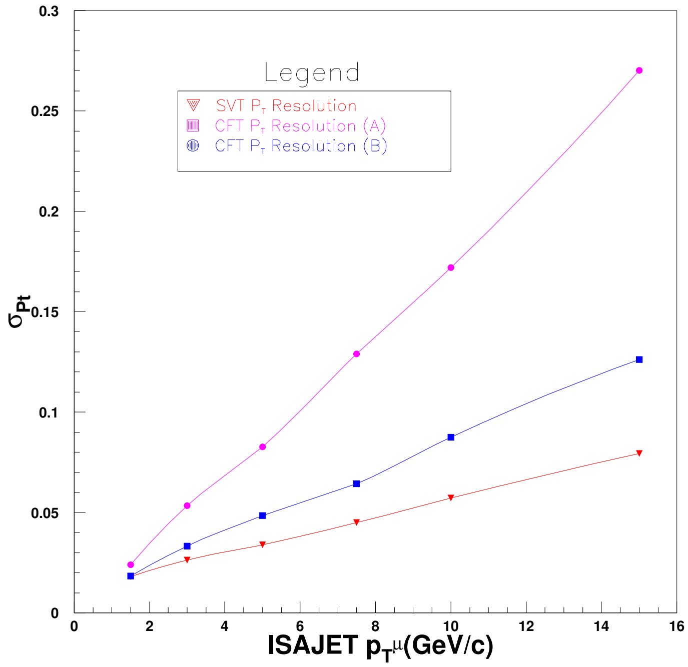

Figure 1: Transverse momentum resolution for muons in single track events; transverse momentum calculated three different ways: CFT momentum (a) (squares), CFT momentum (b) (circles), momentum calculated using SMT and CFT information (triangles)

Figure 1 shows that the resolution using STT improves compared to that obtained using only the CFT information.

- for $p_T = 3$ GeV: $\frac{\sigma(STT)}{\sigma(CFT(a))} \approx 0.5$, $\qquad \frac{\sigma(STT)}{\sigma(CFT(b))} \approx 0.8$

- for $p_T = 15$ GeV: $\frac{\sigma(STT)}{\sigma(CFT(a))} \approx 0.3$, $\frac{\sigma(STT)}{\sigma(CFT(b))} \approx 0.6$

E_T/p_T for electrons at L2:

Fig. 2 shows a comparison of E_T/p_T for electron tracks, with p_t calculated in the three different ways mentioned above. It can be seen that using the STT improves the E_T/p_T resolution by a factor of 2 for high

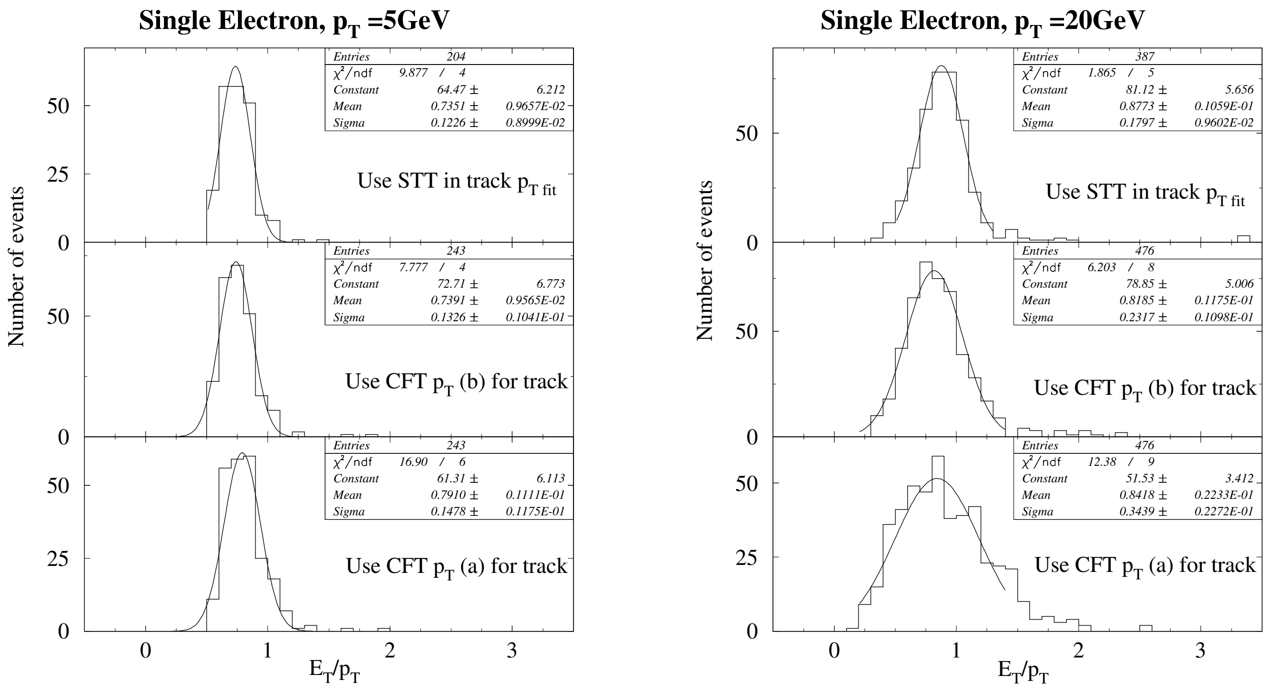

Figure 2: E_t/p_t for electrons with $p_t = 5$GeV (left) and $p_t = 20$GeV (right), assuming a calorimeter energy resolution of $13\%/E$.

p_T electrons compared to CFT(a). This leads to improved rejection and efficiency relative to the 'standard isolated electron' definition, summarized in Table 2.

Table 2: Background rejection and efficiency of E_T/p_T matching relative to the standard isolated electron definition

	$p_T(ele) = 20$ GeV		$p_T(ele) = 5$ GeV	
p_T type	Eff. (%)	Bkg Rej.	Eff. (%)	Bkg Rej.
CFT(a)	90	x3	99	x2
STT+CFT	87	x5	99	x8

Impact Parameter Resolution:

The dependence of the impact parameter resolution on the track p_t was also studied with single pion samples (p_t from 2 to 15 GeV). It was found that the resolution is $\sim 15\ \mu$m at $p_t = 15$ and $\sim 35\ \mu$m at 2 GeV. The p_t dependence of the resolution was parameterized as

$$\sigma_B^2 = \sigma_0^2 + (\frac{\alpha_{ms}}{P_T})^2,$$

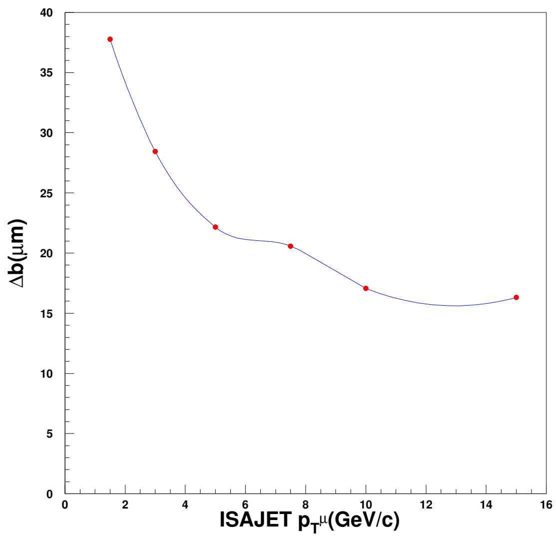

Figure 3: Impact parameter resolution vs p_t, for μ's in single track events

with $\sigma_0 = 12.6$ μm, and $\alpha_{MS} = 49.7$ (GeV/c) $\cdot$ μm. It was found that this same parameterization of the impact parameter resolution vs p_t is also valid for tracks from the primary vertex in $b\bar{b}$ and $t\bar{t}$ events.

The *Impact parameter significance,*

$$S_B = \frac{B}{\sigma_B(p_T)},$$

was determined in the trigger simulation algorithm for every track, using the parameterization of $\sigma_B(p_T)$ mentioned above.

As can be seen in Fig. 4, the distribution of impact parameter significance for tracks coming from the primary vertex is satisfactorily described by a Gaussian for both $b\bar{b}$ and $t\bar{t}$events, although there are non–Gaussian tails. The width is very close to 1 for $b\bar{b}$ events, with a slight degradation and more pronounced tails in $t\bar{t}$ events, due to the high track multiplicity. Furthermore, in both $b\bar{b}$ and $t\bar{t}$ events, the impact parameter significance distribution for tracks from the primary vertex is significantly narrower than that for all tracks (see Fig.5), while it is wide for tracks from b decays (Fig.6).

1.3 Physics benefit studies

In order to assess the physics benefit of the STT trigger for a given physics signal of interest, we first use a set of trigger conditions (both L1 and L2) which do not use the SMT information, i.e. are only based on the calorimeter, muon and CFT triggers. We then vary these trigger conditions to optimize signal efficiency and background rejection, while trying to maintain trigger rates which are compatible with the available bandwidth. Then we check whether additional use of SMT information at L2 allows better signal efficiency for the same total trigger rate, or allows a reduction of the trigger rate while maintaining the efficiency.

The additional handles made available due to an STTpp that can be used in a L2 trigger decision include:

- maximum p_t
- number of tracks with p_t above some threshold
- maximum impact parameter
- maximum impact parameter significance

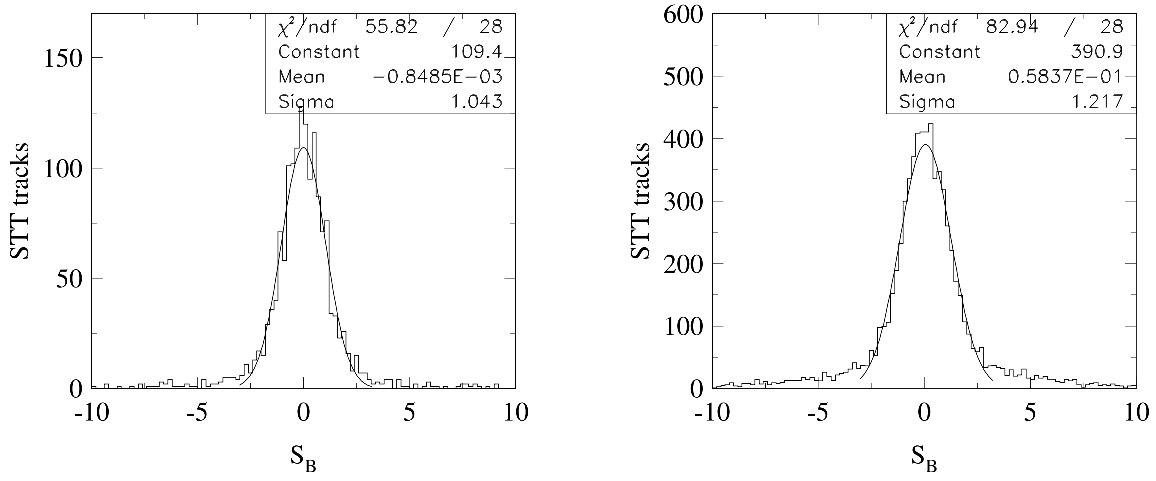

Figure 4: Impact parameter significance distribution for tracks matched to MC tracks coming from primary vertex, for $b\bar{b}$ events (left), and for $t\bar{t}$ events (right)

- number of tracks with impact parameter above some threshold
- number of tracks with impact parameter significance above some threshold.

In the following we describe briefly the physics benefits that could be derived from using the additional handles provided by the STT. It will be shown that the STT as proposed could bring improvements for $t\bar{t}$ and single top studies, for Higgs searches and for B physics. In addition it will allow to record a sample of $Z \rightarrow b\bar{b}$ events which can be used for b jet energy calibration. Finally, it offers the possibility of determining the z position of the primary vertices at L2, which can be used at L3 to sharpen the E_t thresholds when triggering on electrons and jets.

1.4 $t\bar{t}$

In the Standard Model with three generations, existing experimental constraints and the unitarity of the CKM matrix require $\mid V_{tb} \mid \simeq 1$, predicting that the weak decay of the top proceeds almost exclusively through W + b. The $t \rightarrow Wb$ decay vertex is completely fixed by the universal V − A coupling to the SU(2) bosons. The decay width is given by [23]

$$\Gamma(t \rightarrow bW^+) \quad = \quad \frac{G_F m_t^3}{8\sqrt{2}\pi} |V_{tb}|^2 [1 - \frac{m_W^2}{m_t^2}]^2 [1 + 2\frac{m_W^2}{m_t^2}]$$

For $m_t = 170$ GeV/c^2, this partial decay width is ~ 1.8 GeV, corresponding to a lifetime of $\sim 0.4 \times 10^{-24}$ seconds. This rapid decay cuts off the long distance part of the strong interaction; there is no hadronization, and all strong interaction issues for the top quark should be well described by perturbative QCD. Nature provides a tool which does not exist for the light quarks: a two body weak decay which precedes hadronization and therefore carries helicity information related to the fundamental couplings. Because the top is heavy, it is possible that the physics of an underlying theory at a high mass scale may manifest itself via new non-universal top interactions [24]. The top quark provides the first opportunity to study the decays of a naked quark, with experimental techniques and advantages familiar from muon decay.

The top quark has been discovered at the Tevatron [18, 19] in its dominant production mode, strong production of $t\bar{t}$ pairs [20]. In addition, a single top quark can be produced via the electroweak interaction [22]. The event yield with and without a STT strongly depends on the bandwidth allocation for top physics

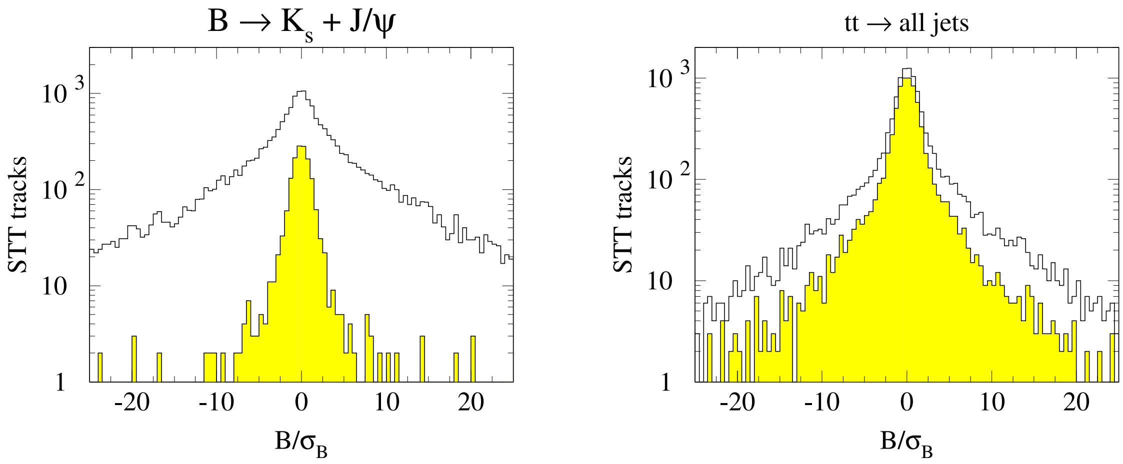

Figure 5: Impact parameter significance distribution for matched tracks, for $B \to K_s + J/\psi$ events (left) and $t\bar{t} \to$ ***all jets*** events (right); the shaded histogram corresponds to tracks from the primary vertex.

during Run II. If the bandwidth for top physics is significantly restricted, the gain from a STT will be larger, since it will help fit the top events into the available bandwidth.

To study the benefits of the STT for the selection of $t\bar{t}$ events, two samples of events generated by ISAJET and processed with the FEB97 version of UPG_GEANT were used:

- a sample of 2126 events in which both W's decay into hadrons, denoted as $t\bar{t} \to$ ***all jets***;
- a sample of 1175 events in which one of the W's is forced to decay into a muon+neutrino final state, and denoted as $t\bar{t} \to \mu +$ ***jets***.

We start out by looking for "standard" triggers (i.e. without STT) which have a high efficiency for $t\bar{t}$ events. The most promising ones with their definitions, background rates, as well as efficiencies for $t\bar{t}$ events are shown in Table 3.

From the observed differences in the S_B distributions between primary tracks and tracks from b decays (see Figs. 5 and 6) we expect that imposing conditions on S_B will reduce the background more than the signal. This is demonstrated in Fig. 7 for one of the triggers (JET2MED) and for the $t\bar{t} \to$ ***all jets*** sample. Very similar results were obtained for the $t\bar{t} \to \mu +$ ***jets*** events. About 8% of the events are lost when requiring at least 1 STT track due to the limited acceptance of the SMT along the z axis. Efficiency well above 80% is obtained when requiring only one track with a large impact parameter significance.

Fig. 7 also shows that the trigger rate can be reduced by a factor of ~ 2 when requiring at least 1 track with a significance greater than 3, and a reduction factor of 4 is reached when at least 2 tracks with $\mid S_B \mid > 3$ are requested. The $t\bar{t} \to$ ***all jets*** trigger efficiencies corresponding to these two criteria are 86.9% and 77.7%, respectively.

A 30 μm uncertainty on the primary vertex position leads to a 5% reduction of the signal efficiency for a fixed JET2MED background rate of 20 Hz. A systematic shift of the primary vertex position in the transversal plane limited to 100 μm does not introduce a signal efficiency loss as long as the STT criterion is adapted to maintain the background rate at a constant level (see ref. [2]).

The background rates and signal efficiencies obtained for various trigger configurations with and without STT are compiled in Table 3. The STT condition consists in requiring at least two tracks with $\mid S_B \mid > 2.5$. The combination $\Sigma\,(1 \to 3)$ based on calorimeter-only triggers gives efficiencies of 86% and 96.2% for the signal samples with a background rate of 7.2 Hz at L2. To reach efficiencies close to 100% for both the $t\bar{t} \to \mu +$ ***jets*** and $t\bar{t} \to$ ***all jets*** events, it is necessary to use a combination of 5 or 6 of the

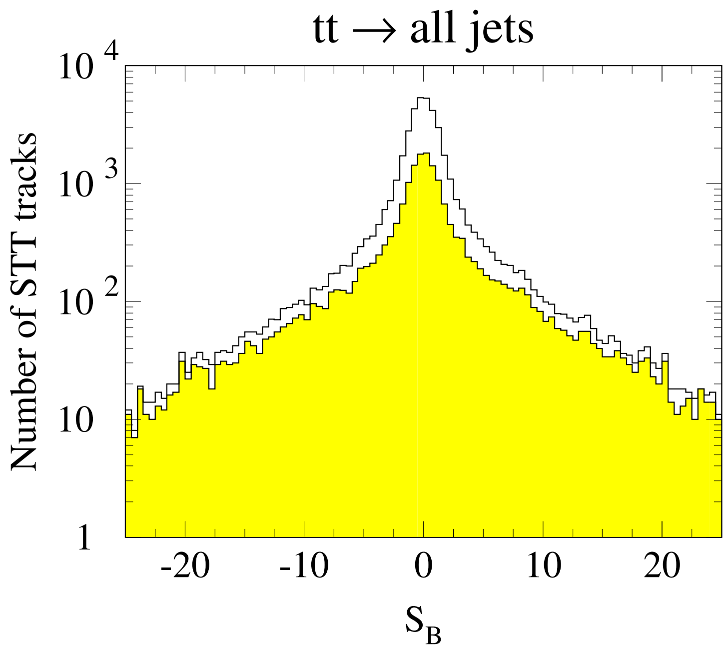

Figure 6: Impact parameter significance distribution for tracks matched to MC tracks in $t\bar{t} \rightarrow$ *all jets* events; the shaded histogram corresponds to tracks coming from b-quark decays.

base triggers but the corresponding background rates increase to about 110 Hz. The trigger combination $\Sigma(1 \rightarrow 3) + \Sigma(4 \rightarrow 6) \times STT$ allows then a reduction by a factor 3 of this background rate without significantly affecting the signal efficiencies. This combination allows to reach better signal efficiencies than the combination $\Sigma(1 \rightarrow 3)$ while keeping background rates well below 100 Hz.

1.5 Single top production

The single top process presents an interesting laboratory for study of the top quark. During Run I this very important production mode was inaccessible since the integrated luminosity was not high enough [21]. At $m_t = 170$ GeV/c^2 the Tevatron Run II with integrated luminosity of 2 fb^{-1}will produce approximately 4K single top events [22].

The coupling between a W-boson and top and bottom quarks has not yet been studied directly. Top quark pair production is not a good process for probing the CKM matrix element V_{tb} since this production proceeds via a gtt vertex. Information about Wtb coupling from top quark decay is relatively inaccessible in $t\bar{t}$production because the width of the decay into Wb is proportional to the branching fraction of $t \rightarrow Wb$, which is ≈ 1 in the standard model ($0.9991 \leq | V_{tb} \leq 0.9994$ at 90%C.L. [25]). Single top quarks are produced at hadron colliders mainly from a Wtb vertex, and thereby provide a direct probe of the nature of the Wtb coupling and of the CKM matrix element V_{tb}.

The important measurements to be done with the sample of single top events include:

- The single top cross section, which is proportional to $\Gamma(t \rightarrow Wb)$.
- Branching ratio of top to left-handed vs. longitudinally polarized W's. They depend on the top quark a mass and the W boson mass. Non-universal top couplings will, in many cases, appear as a departure

Table 3: Background rates and $t\bar{t}$ trigger efficiencies

	Background (Hz)			$tt \to \mu + jets$ (%)		$tt \to all\ jets$ (%)	
Trigger	L1	L2	L2+STT	L2	L2+STT	L2	L2+STT
1–JMULT	49.1	2.1	0.8	27.4	22.3	69.8	58.5
2–MJTMET	55.2	3.3	1.0	68.5	55.1	48.7	38.6
3–JMAX	49.7	13.0	6.3	68.3	55.7	84.2	69.7
4–MUJET	64.1	41.6	8.1	74.3	58.5	53.2	42.4
5–JET2MED	186	85.2	24.2	88.3	70.9	98.3	80.2
6–MUMAX	13.0	6.5	3.4	51.6	42.0	14.3	10.9
7–$\Sigma\,(1 \to 3)$	82.5	17.2	7.2	86.0	69.1	96.2	78.3
8–$\Sigma\,(1 \to 5)$	239	113	28.5	96.1	76.0	99.8	81.1
9–$\Sigma\,(1 \to 6)$	248	118	31.3	97.2	76.8	99.8	81.1
10–$\Sigma\,(1 \to 3)+$ $\Sigma(4 \to 5) \times STT$	239	113	38.5	96.1	92.9	99.8	98.6
11–$\Sigma\,(1 \to 3)+$ $\Sigma(4 \to 6) \times STT$	248	118	41.3	97.2	93.7	99.8	98.6

JMULT	≥ 4 jets with $E_T \geq 15$ GeV
MJTMET	≥ 3 $E_T^{jet} \geq 10$ GeV + missing $E_T \geq 20$ GeV
JMAX	≥ 1 jet with $E_T \geq 45$ GeV
MUJET	≥ 1 $p_T^{\mu} \geq 6$, $E_T^1 \geq 20$ GeV and $E_T^2 \geq 10$ GeV
JET2MED	≥ 2 jets with $E_T \geq 20$ GeV
STT	at least 2 tracks with $\mid S \mid \geq 2.5$

from the expected value.

- Measurement of $|V_{tb}|$.
- A single top will be produced with almost 100% left-handed polarization. This polarization allows one to search for CP violation in the decay of the top quark.

The single top production events generated using COMPHEP [17] were processed through the Feb97 version of UPG_GEANT. A combination of electron, muon and jet triggers with high efficiency for single top events (see ref. [8]) was chosen from the standard trigger menu, and the effect of additonal STT conditions on signal efficiency and background rejection was examined.

The main findings are summarized in Tables 4 and 5. It is found that in both leptonic and hadronic decay modes of the W, the additional handle provided by the STT allows a reduction of the L2 trigger rate, with little loss in signal efficiency. Using the STT may become indispensible if it turns out that the background rates are underestimated by the simulation.

1.6 Higgs search

A major question facing particle physics is understanding the mechanism for electroweak symmetry breaking. The current, unconfirmed, view is that the neutral Higgs boson plays a significant role. Given this, it is obvious that a Higgs search should be a significant component of an experimental program if at all possible. The current lower bound on the Higgs mass is 89 GeV[27] and is expected to reach approximately 105 GeV [28] by the end of the LEP II running. Theoretical constraints on the Higgs are weak, but favor masses below 150 GeV.

The LHC experiments are being designed specifically for Higgs searches with mass sensitivity between 90 GeV and 1 TeV. However, these experiments have sensitivity to Higgs of mass less than 130 GeV only

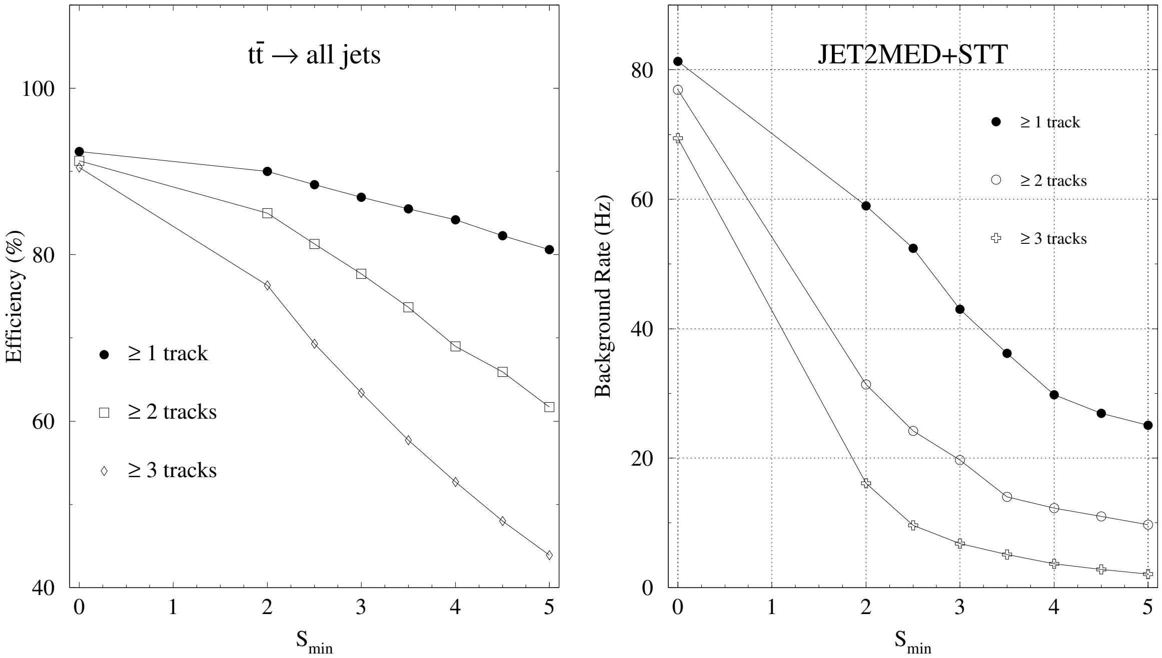

Figure 7: $t\bar{t}$: Signal efficiency for $t\bar{t} \rightarrow$ ***all jets*** events (left) and QCD background rate for the events satisfying the L2 JET2MED trigger together with a STT trigger (condition: 2 tracks with $|S_B| \geq S_{min}$)

through the experimentally challenging $H \rightarrow \gamma\gamma$ signature. Even if an excess is observed in this channel, interpreting these results will be very difficult.

The prospect for Higgs searches during the Tevatron run II and TeV33 eras has been outlined elsewhere[29][30]. For run II a factor of 10 improvement over that discussed in the studies would be needed to find a 100 GeV higgs boson. These studies considered only the canonical discovery mode, $p\overline{p} \rightarrow WH^0 \rightarrow l\nu b\overline{b}$, but the bulk of the cross section times branching ratio for WH^0 and ZH^0 lies in purely hadronic decay modes. For WH^0 production, 67% of the decays are to $q\overline{q}b\overline{b}$. For ZH^0 production 70% of the events decay to $q\overline{q}b\overline{b}$. It is clear that sensitivity in these channels would significantly enhance the viability of Higgs searches in run II.

In the past, specific channels were allotted trigger bandwidth using a priority determined by a DØ trigger board. For a speculative but important analysis like the higgs search, a trigger rate of 2-3% of the total available bandwidth has arbitrarily been chosen as the goal.

For this study [4], a sample of 1700 $p\overline{p} \rightarrow WH^0 \rightarrow q\overline{q}b\overline{b}$ events were generated using Pythia V5.7 with $M_H = 90$ GeV. The events were passed through the August '96 version of UPG_GEANT and the standard run II trigger–simulation package[10, 11]. No additional min-bias interactions were added to this sample. As in the $t\bar{t}$ case, we first look for a set of standard triggers so as to maximize efficiency for the signal, the hadronic decay of the Higgs Boson. Some of the triggers that were considered are shown in Table 6.

From this table, one sees that all of the triggers which meet the target bandwidth of 2-3% for L1 and L2 have signal efficiencies below 50%. For searches it is critical to maintain as much efficiency as possible, so these triggers are not particularly desirable. The trigger JET_3_MED has acceptable L1 rates and significantly better signal efficiency, but the L2 rate is somewhat high. Additional trigger conditions using track information offer a possibility to reduce the trigger rate while maintaining acceptable signal efficiency. This is summarized in Table 7 and Fig. 8. It can be seen that for relative trigger efficiencies of

Table 4: Single top production: Summary of background rejection and single top signal efficiency for three trigger classes, augmented by an STT condition at L2; the STT condition is at least one track with $|S_B| \geq S_{min}$.

	rejection beyond L2		efficiency relative to L2	
	$S_{min} = 2$	$S_{min} = 4$	$S_{min} = 2$	$S_{min} = 4$
electrons	1.6	3.0	87%	74 %
muons	1.4	7.0	90%	78 %
jets	1.4	3.0	94%	80 %

Table 5: Background rates at L1 and at L2 for single top triggers, with and without additonal STT condition ($|S_B| \geq S_{min}$) at L2; "TT" means "trigger tiles".

Trigger		L1	L2	L2 rates with STT	
L1	L2	rates	rates	$S_{min} = 2$	$S_{min} = 4$
cent. e (7 GeV)	cent. e(7 GeV)	105	45	21	17
e (7 GeV) + 2 TT (7 GeV)	e (7 GeV) + 2 jets (7 GeV)	136	36	22	11
single μ (7 GeV)	single μ (7 GeV)	13	7	5	1
5 TT $\geq$ 3 GeV	2 jets $\geq$ 15 GeV	180	117	73	40
6 TT $\geq$ 3 GeV	2 jets $\geq$ 15 GeV	66	60	43	25
2 TT $\geq$ 5 GeV	2 jets $\geq$ 15 GeV	620	265	152	76

90%, the raw calorimeter trigger rate can be reduced by a factor of two to three, and that the use of STT information increases the rejection by 25% over the best non-STT trigger. As the trigger efficiency drops, the effect of STT information becomes much more significant. At a relative efficiency of 80%, the STT triggers have rejection which is a factor of 1.5 better than the CFT–based triggers. For a relative efficiency of 50%, the STT triggers have rejection factors of up to 40, while the CFT trigger rejection is only a factor of 10. The best algorithm is that which requires at least N STT tracks having $p_T \geq 3' \, GeV$. Triggers which use STT information have significantly better performance than those which use only CFT information.

In conclusion, we find that for a the dominant decay signature for associated production of a 90 GeV Higgs Boson in the modes WH^0 and ZH^0, a calorimeter plus CFT trigger could have 68% overall efficiency with a L1 rate of 200 Hz and a L2 rate of 20 Hz. The efficiency of the calorimeter portion of the trigger is 74%, while the track portion has an efficiency of 90%. With the help of the STT, the rejection can be improved by an additional 25%. For tracking–only efficiencies in the range 50% to 85%, the STT trigger gives factors of 4× to 1.5× better rejection than the best trigger without using SMT information. From these results, it is clear that a silicon track trigger can significantly help in the $W/Z + H^0$ search.

1.7 $Z \rightarrow b\bar{b}$

Reconstructing a $Z \rightarrow b\bar{b}$ signal in Run II could be quite important. It would provide proof that a resonance decaying to $b\bar{b}$ can be reconstructed and give a measurement of the $b\bar{b}$ invariant mass resolution, thereby giving credibility to searches for new particles that decay to $b\bar{b}$. This is the primary decay mode of the Higgs boson in the mass range accessible to the Tevatron [29]. In SUSY and technicolor theories [31] there may also be particles that decay to $b\bar{b}$. A measurement of the position of the invariant mass peak also would cross check the jet energy scale calibration, which is the largest systematic uncertainty in the top quark mass measurement. The decay $Z \rightarrow b\bar{b}$ provides the best chance to reconstruct a narrow resonance decaying to jets, because the b quark decays allow flavor tagging for the final state jets and therefore rejection against the overwhelming background from continuum gluon jet production. As we will show the large gluon jet

Table 6: Higgs search: Trigger definitions, background rates(r) and signal efficiencies(ϵ) for the pure calorimeter triggers. The total bandwidth is expected to be 10 kHz for L1 and 1 kHz for L2.

	Calorimeter	Cal. Thresholds	L1		L2	
Trigger	Multiplicity	(L1,L2), GeV	r (Hz)	ϵ(%)	r(Hz)	ϵ(%)
JET_3_LOW	3	(3,5)	2000	100	140	78
JET_3_MED	3	(5,10)	200	91	63	74
JET_3_HIGH	3	(7,15)	52	71	15	52
JET_4_LOW	4	(3,5)	670	98	13	36
JET_4_MED	4	(5,10)	58	78	6	34
JET_4_HIGH	4	(7,15)	17	51	1	17
JET_5_LOW	5	(3,5)	250	93	2.0	8
JET_5_MED	5	(5,10)	24	62	0.1	8
JET_5_HIGH	5	(7,15)	5	32	0.04	3

background makes it impossible to trigger efficiently on $Z \rightarrow b\bar{b}$ decays without flavor tagging.

For this study [6] we use $Z \rightarrow b\bar{b}$ events generated with ISAJET, 9979 of which have no additional minumum bias events, 995 are overlayed with 2, and 992 with 5 additional minimum bias events. These events were processed by the UPG_GEANT program (release version FEB97).

Using the fact that most of the $Z \rightarrow b\bar{b}$ events have at least two jets with E_T above 20 GeV, we define a set of calorimeter-based triggers which require the presence of at least two hadronic towers in the calorimeter at Level 1 and and also two clustered jets at Level 2 above a certain E_T threshold. The definitions of these triggers, as well as rates and efficiencies for $Z \rightarrow b\bar{b}$ are summarized in table 8. One sees that for 40% L2 efficiency the L2 rate is about 25% of the available bandwidth, which is unacceptably high, and even for 20% efficiency the L2 rate corresponds to an uncomfortably high 8.5% of the bandwidth.

To control the rate, tracking information at the trigger level can be used. Table 9 and Fig. 11 demonstrates the effect of using CFT information in addition to the calorimeter. From the curve as well as the table we note that for an acceptable efficiency of 35% out of Level 2, the background rate still remains at about 20% of the bandwidth. By comparing JET_2_MED_T3 from table 9 to JET_2_MED in table 8 we note that the CFT requirement of two tracks with p_T above 3 GeV gives a factor of 1.4 background rejection for a 15% loss of efficiency. For a 50% loss in efficiency we expect a background rejection factor of 2.5.

It is clear from the above discussion that given the present trigger scheme the $Z \rightarrow b\bar{b}$ trigger will be heavily prescaled and it is questionable if we can record enough events to see a signal.

Using the impact parameter information provided by the STT provides a much more powerful handle for background rejection, as shown in Figs. 9 and 11 and Table 10. We find, e.g., that by using the STT one gains a factor of 2 in background rejection compared to the CFT based JET_2_MED_T2 trigger, for the same overall efficiency of 35%. For a background rate of as low as 20 Hz, we still have a final efficiency of around 20%. This is a factor of 5 increase in efficiency compared to the calorimeter based JET_3_MED trigger which gave the same low background rate. Thus, adding the Silicon Track Trigger at Level 2 gives us the capability of triggering on $Z \rightarrow b\bar{b}$ events at a low rate while maintaining an acceptable efficiency.

In conclusion, we have shown that we can reduce the trigger rate at Level 2 to 20 Hz at an efficiency of 20% for $Z \rightarrow b\bar{b}$. Assuming this trigger efficiency, we estimate the expected signal and background yields for a 1 fb^{-1} data set: The number of reconstructed events is given by

$$N = \sigma \epsilon_1 \epsilon_2 \int \mathcal{L} dt, \tag{1}$$

where σ is the cross section for the process considered, ϵ_1 the trigger efficiency, ϵ_2 the reconstruction efficiency, and $\mathcal{L}$ the luminosity. Table 11 lists the relevant numbers for signal and background. The value for ϵ_2 is a guess of the additional efficiency of an offline double b tag. Even with the pessimistic assumption of 25% efficiency for the signal and only a factor 10 rejection for background we get signal/$\sqrt{\text{background}} \approx 17$.

Table 7: Higgs search: Representative background rates and rejections for four (arbitrarily chosen) signal efficiencies for the different trigger types. The lower part of the Table gives a definition of the different STT conditions considered. The good tracks are ordered separately by b and S, and an index i or j denotes the track rank. The ranking is by p_T, with the highest p_T track first.

Trigger Type	Background Rejection			
	$\epsilon \approx 90\%$	$\epsilon \approx 80\%$	$\epsilon \approx 50\%$	$\epsilon \approx 10\%$
N CFT tracks w/$p_T \geq 3$ GeV	2.5	4.7	10	35
N STT tracks w/$p_T \geq 3$ GeV	3.1	7.5	40	1000
N STT tracks w/$b \geq 30$ μm	2	3.8	27	900
N STT tracks w/$S \geq 2$	2	5.5	30	300
Event $\|b\|_{25} \geq X$	2.2	3.8	21	300
Event $S_{25} \geq X$	2.0	5	27	200
N CFT w/$p_T \geq 3$ and $\overline{b_{25}} \geq X$	3.0	6.4	26	500
N w/$p_T \geq 3$ and $\overline{S_{25}} \geq X$	2.8	7.1	33	650

Name	Description
$\|b\|_i,\ i = 1,5$	The impact parameter of the i-th track
$S_i,\ i = 1,5$	The impact parameter significance of the i-th track
$\overline{\|b\|}_{ij}$	The average impact parameter of tracks i through j.
$\overline{S}_{ij}$	The average impact parameter significance of tracks i through j.

1.8 B-physics

With the commissioning of the B Factory at SLAC and the upgraded CLEO detector, B physics will be intensively studied during the years of Run II. Hadron colliders can play a role in these investigations. The areas of B physics that will be of intense interest are:

- B_s mixing
- CP Violation
  - Measure of $\sin(2\alpha)$ with the $B \to \pi^+\pi^-$ decay mode
  - Measure of $\sin(2\beta)$ with $B \to J/\psi K_s$
  - Search for CP violation in $B_s \to J/\psi\phi$
- Search for rare decay modes
  - $B \to \ell\ell X_s$
  - $B_s \to \ell^+\ell^-$ or $B_d \to \ell^+\ell^-$
- Measure of $\Delta\Gamma_s/\Gamma_s$ with $B_s \to J/\psi\phi$ and $B_s \to D_s\ell\nu$.
- Radiative B decays (*e.g.* $B \to \rho\gamma$)
- Measures of V_{ub} and V_{cb} with semileptonic decay channels

Table 8: Trigger rates and efficiencies for $Z \to b\bar{b}$ using calorimeter based triggers only. The trigger definition is given in the second column where n(L1,L2) represents "n" towers in Level 1 and and "n" jets in Level 2 with E_T greater than (L1, L2) GeV respectively. The efficiencies ϵ_1, ϵ_3 and ϵ_6 correspond to $Z \to b\bar{b}$ events with 0, 2, or 5 additional minbias events overlayed, respectively.

	Cal	L1				L2			
Trigger	n(L1,L2)	r(Hz)	ϵ_1(%)	ϵ_3(%)	ϵ_6(%)	r(Hz)	ϵ_1(%)	ϵ_3(%)	ϵ_6(%)
JET_2_MIN	2(3,10)	8028	82	85	85	1390	67	72	75
JET_2_MED	2(5,15)	621	56	59	58	264	41	47	49
JET_2_MAX	2(7,20)	186	32	34	34	85	20	23	27
JET_3_MIN	3(3,10)	1502	68	72	74	132	9	11	16
JET_3_MED	3(5,15)	167	31	34	34	25	4	5	6

Table 9: Trigger rates and efficiencies using Calorimeter and CFT.

	Cal/CFT	L1				L2			
Trigger	n(L1,L2)+(n,p_T)	r(Hz)	ϵ_1(%)	ϵ_3(%)	ϵ_6(%)	r(Hz)	ϵ_1(%)	ϵ_3(%)	ϵ_6(%)
JET_2_MIN_T2	2(3,10)+(2,3)	2389	67	72	75	866	57	62	66
JET_2_MIN_T3	2(3,10)+(3,3)	1319	57	62	69	541	50	55	62
JET_2_MED_T2	2(5,15)+(2,3)	450	48	51	52	201	35	41	43

The B production cross section at the Tevatron is large. The challenge at a hadron collider is isolating the most interesting B physics from the copious backgrounds. Due to the event rate and bandwidth limitations in the DAQ system, it is desirable to achieve as high as possible signal-to-background at the trigger level. For B physics, this is best accomplished using silicon tracking information to exploit the long lifetime of B hadrons.

These physics topics must be considered within the context of the upgraded trigger and data aquisition system. Since an impact parameter device would reside at the second level of the trigger, any physics process must emerge through the Level 1 bandwidth (≈10 kHz) before improving the signal-to-background with the silicon tracking information. This constraint eliminates the possibility of triggering on all hadronic decay modes of the B hadrons. However,many of the processes depend on a leptonic decay mode such as a single muon or dimuon. Therefore, to understand the impact on B physics, we concentrate on the effect of an impact parameter trigger on the dimuon and single muon events at Level 2.

Table 10: L2 trigger rates and efficiencies for $Z \to b\bar{b}$, with CFT and with STT; "STT(a)" corresponds to STT conditions adjusted so as to keep the overall signal efficiency 35%, while "STT(b)" corresponds to conditions which keep the background rate at 20 Hz.

	Cal/CFT		STT(a)		STT(b)	
Trigger	r (Hz)	ϵ(%)	r(Hz)	ϵ(%)	r(Hz)	ϵ(%)
JET_2_MIN	1390	67	60	35	20	19
JET_2_MED	264	41	110	35	20	23
JET_2_MIN_T2	866	57	62	35	20	20
JET_2_MIN_T3	541	50	77	35	20	19
JET_2_MED_T2	201	35				
JET_3_MED	25	4				

Table 11: $Z \to b\bar{b}$: Signal and Background Yields for $\int \mathcal{L}dt = 1$ fb^{-1}.

process	σ	ϵ_1	ϵ_2	N
$Z \to b\bar{b}$	1 nb	20%	25%	5×10^4
background	100 nb	100%	10%	10^7
*****	?	?		

A very detailed study of triggering for B-physics [7] considered various samples:

1. $B_d^o \to K_s^o + J/\psi$, $J/\psi \to \mu^+\mu^-$ (CP asymmetry)
2. $B_s^o \to D_s^- + 3\pi^\pm$, $D_s^- \to K^+K^-\pi^-$ (B_s mixing)
3. $B_s^o \to D_s^- + \mu^+ + \nu_\mu$, $D_s^- \to K^+K^-\pi^-$ (B_s mixing),

where in the B_s samples the B on the other side was forced to decay into $\mu + X$, giving at least one muon to trigger on.

Table 12: B physics:Background rate and signal efficiency for various muon triggers. Muon trigger code has two letters and one number; 1st letter: region covered (C – $|\eta| \leq 1$, X $|\eta| \leq 2$), 2nd letter: tag condition (L – loose, M – medium, T – tight), number: p_t threshold (1 – 2GeV, 2 – 4GeV, 3 – 7GeV). "STT(2.5)" means at least one track found by STT with $|S_B| \geq 2.5$.

Trigger	Bgd. (Hz)	$K_s + J/\psi$ (%)	$D_s^- + \mu^+$ (%)	$D_s^- + 3\pi^\pm$ (%)
dimuon				
• (CM1,CM2)	1.3	10.2	3.3	0.0
• (CT1,CT2)	272	20.1	8.2	0.5
• (CT1,CT1) + $E_T^{jet} > 10$GeV	102	0.9	0.5	0.0
• (CT1,CT1) +STT(2.5)	7.6	14.9	5.5	0.3
single muon				
• XM2	38.6	23.9	11.8	4.6
• XM3	13.5	10.8	4.4	1.4
• XM2+CFT	21.0	13.5	5.7	2.0
• XM2+STT(2.5)	13.2	17.3	7.3	2.5
• XM2+STT(3.5)	5.6	16.0	6.2	2.0
$\mu\mu + \mu$ trigger combinations				
• XM2.OR. (CT1,CT1)+STT(2.5)	45.0	31.9	15.6	4.9
• (XM2.OR.(CT1,CT1)) +STT(2.5)	19.6	25.2	11.0	2.7
• (XM2.OR.(CT1,CT1)) +STT(3.5)	11.5	23.2	9.2	2.2

The benefits that would result from the use of a Silicon Track Trigger at L2 are summarized in Table 12 and demonstrated in Fig. 12. The main conclusions are:

- The STT provides a better background rejection than the CFT while preserving a better signal efficiency.

- An STT would allow to reduce the XM2 (see the caption of Table 12 for definition) background rate by a factor 10 while preserving 70% of the reconstructable $Q\bar{Q}$ events. This result is marginally affected when a 30 μm smearing of the primary vertex position is taken into account.

- For the dimuon triggers, it would permit a reduction to 2 GeV/c of the p_T threshold on both muons, enriching the sample of signal events by 75% ($B \to K_s + J/\psi$) to 95% ($B_s^\circ \to D_s^- + \mu^+ + \nu_\mu$) compared to the (CM1,CM2) trigger and keeping the background rate as low as 10 Hz. If the XM2 background rate turns out to be acceptable, the trigger combination XM2.OR.[(CT1,CT1)+STT] allows a 33% increase of the trigger efficiency for $B \to K_s + J/\psi$ and $B_s^\circ \to D_s^- + \mu^+ + \nu_\mu$ events with respect to XM2 alone. This efficiency gain is accompanied by a moderate 16% increase of the background rate. The best compromise between background rate and efficiency is probably obtained with the combination [XM2.OR.(CT1,CT1)] +STT(2.5), which provides a 25.2% efficiency for $K_s + J/\psi$ events and leads to a background rate of 19.6 Hz, representing 2% of the L2 bandwith.

- The STT would also be very useful to control the rate of a low threshold dielectron trigger, allowing the collection of low p_T $J/\psi \to ee$ events for calibration and physics analysis purposes.

- An efficient single muon trigger with $p_T \geq 4$ GeV/c is our only chance to search for B_s mixing up to $x_s = 20$ and to determine $\sin 2\beta$ with a competitive precision; an STT would offer the possibility to have such a trigger, with acceptable background rates.

In summary, for all trigger configurations of interest for B-physics, a Silicon Track Trigger would represent a powerful tool to reduce the background rates. From the physics analysis point of view, it would be more effective than a simple blind prescaling.

1.9 z_{vertex} determination

Currently the Level 3 system for Run II is allocated a 25 ms time budget for reconstructing an event in a L3 node. It is not clear whether there is enough time to unpack the hits from the Silicon Vertex Detector and use them to implement a fast z-vertex finding. If this is not feasible then it would be advantageous to compute the z-vertex at Level 2 in hardware and pass it along to Level 3 for use in further computations of global quantities, e.g. the E_T of jets and electrons. Knowledge of the z-vertex position at Level 3 is extremely beneficial. During Run I, the Level 2 electron algorithm used the "slow z" position from Level 0 in order to get a better estimate of the electron E_T.

Using the hits in the 90° stereo view of silicon ladders in layers 1 and 3 of the inner four barrel segments of the SMT offers the possibility to determine the z position of the primary event vertex Level 2. An algorithm was found [5] which could be implemented in hardware at L2, and provide the Z_V information at L2 time, to be used either in the global L2 decision or at L3.

The resolution of the z-vertex measurement is found to be 550 μm for events with one high-p_T interaction. For events with 2 additional min-bias events overlayed, the vertex resolution is determined to be 610 μm. For a sample of $Z \to b\bar{b}$ events without additional interactions and in which the event vertex is within $\pm$ 25 cm, the efficiency for reconstructing a vertex in the $Z \to b\bar{b}$ events is found to be 98%. Since there is only one vertex in the event, we always identify the correct vertex as the high-p_T vertex. If we superpose 2 min-bias interactions on these $Z \to b\bar{b}$ events, the efficiency of reconstructing at least one vertex in these events is 99%. The efficiency for identifying the correct vertex as the high-p_T vertex is 78%. In these events there maybe one or more vertices within the acceptance region and we find that the efficiency to reconstruct a vertex in this environment is about 85%.

Due to the limited acceptance of the silicon detector elements with 90° strips, (only four inner barrels out of six), the reconstruction of z-vertices with this method is limited to $\pm$30 cm around the center of the detector. The rms width of the luminous region during Run II is expected to be 25 cm. About 30% of the events have the high-p_T vertex outside this region. For these either no vertex is found or a min-bias vertex inside this acceptance region (reconstructed with 97% efficiency) is incorrectly identified as the high-p_T vertex.

The influence of the knowledge of the vertex position on the E_T trigger turn-on is shown in Fig. 13. Even if the correct vertex position is only found for $|z| < 30$cm (dash-dotted curve in the figure), there still is a significant improvement in the E_T threshold due to the knowledge of the position of the z-vertex. This improvement implies that we can trigger more efficiently with lower rates on single electrons at Level 3.

References

[1] "Benefits of a Silicon Vertex Trigger for $t\bar{t}$ Events", Frédéric Stichelbaut, DØ Note 3312.

[2] Update of the silicon track trigger studies for $t\bar{t}$ events, Frédéric Stichelbaut, DØ note 3444.

[3] "Studies of SVT trigger using SUGRA four b quark signature", Doug Norman, DØ note 3318.

[4] " Towards a Run II Trigger for $p\overline{p} \rightarrow WH^0 \rightarrow q\overline{q}b\overline{b}$", John Hobbs, DØ Note 3321

[5] "Primary vertex finding al Level 2 using the silicon vertex detector", Meenakshi Narain and Sudhindra Mani, DØ note 3338.

[6] "Triggering on $Z \rightarrow b\bar{b}$ events in run II", Meenakshi Narain, DØ note 3339.

[7] "Triggers for B physics in run II", Frédéric Stichelbaut, Andrzej Zieminski, Meenakshi Narain, DØ note 3354.

[8] "Single top and the silicon tracker trigger", Terry Heuring, DØ note 3400.

[9] "Silicon track trigger performance studies", Terry Heuring, Dan Karmgard, DØ note 3415.

[10] private communication: trigger ntuple code by multiple authors (Cecilia Gerber, Phil Gutierrez, Chris Klopfenstein, Meenakshi Narain, Dan Owen, Eric Smith, Kathy Streets, Kin Yip)

[11] Private communication, Jerry Blazey and Cecilia Gerber. See instructions at `http://niuhep.physics.niu.edu/~blazey/ntuple_AUG96.html`

[12] "L1 axial CFT trigger hardware and firmware design for the baseline trigger algorithm, Fred Borcherding", DØ note 3082.

[13] "The impact of a displaced vertex trigger on the CFT L1 axial trigger, Fred Borcherding", DØ note

[14] "Central fiber tracker trigger simulation", Kathy Streets, Kin Yip, DØ note 3301.

[15] "An algorithm for a silicon track trigger", P. Gutierrez, E. Smith, H. Muramatsu, DØ note XXXX

[16] Meena Narain, algorithm and code presented during STT working group meetings.

[17] E. Boos, M. Dubinin, V. Ilyin, A. Pukhov, and V. Savrin, SNUT-94-116, hep-ph/9503280;
A.P. Heinson, A.S. Belyaev, E.E. Boos, *Phys. Rev.* **D56** 3114.

[18] S. Abachi *et al.*, Phys. Rev. Lett. **74**, 2632 (1995).

[19] F. Abe *et al.*, Phys. Rev. Lett. **74**, 2626 (1995).

[20] See, for example, E. Laenen, J. Smith, and W.L. van Neerven, Phys. Lett. **B321**, 254 (1994).

[21] "Status of single top analysis for $e\ +\ jets/\mu$" A. Belyaev *et al.*., DØ note 3441;
Jeff McDonald, private communication.

[22] See, for example, S. Dawson, *Nucl. Phys.* **B249**, 42 (1985); C.-P. Yuan, *Phys. Rev.***D 41**, 42 (1990); R.K. Ellis and S. Parke, *Phys. Rev.***D 46**, 3785 (1992); G. Bordes and B. van Eijk, *Nucl. Phys.* **B435**, 23 (1995).

[23] I. Bigi *et al.*, *Phys Lett.* **B181**, 157 (1986).

[24] For example, see R.S. Chivukula, S.B. Selipsky, E.H. Simmons, *Phys. Rev. Lett.***69**, 575 (1992); D. Carlson, E. Malkawi, C.-P. Yuan, *Phys. Lett.* **B337**, 145 (1994).

[25] Particle Data Group, O. Caso *et al.*., "Review of Particel Physics", *European Physics Journal* **C 3** 1 - 794 (1998).

[26] "Searches for New Particles at Present Colliders", P. Janot, in Proceedings from International Europhysics Conference on High Energy Physics, August, 1997.

[27] "Standard Model Higgs at LEP", Peter McNamara, invited talk at ICHEP98.

[28] "Searching for new particles at existing accelerators", Daniel Treille, invited talk at ICHEP98.

[29] "The TeV 2000 Report", D. Amidei and R. Brock, eds., FERMILAB-PUB-96/082.

[30] "The TEV33 Committee Report", Amidei, *et al.*, Feb. 1996.

[31] E. Eichten, K. Lane, J. Womersley, *Phys. Lett.* **B405**, 305 (1997).

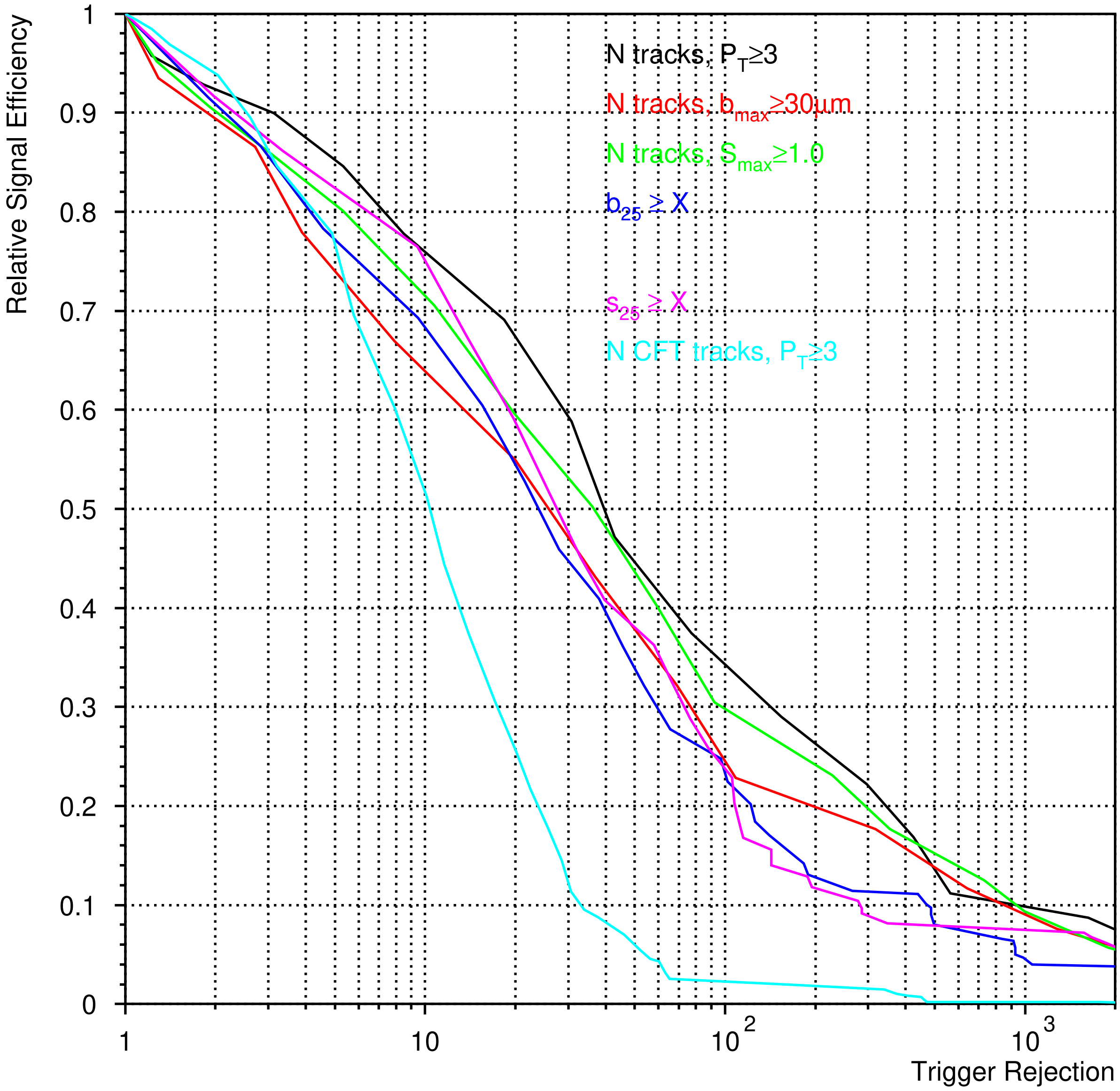

Figure 8: Efficiency versus rejection for the best result from each of the trigger algorithms considered here.

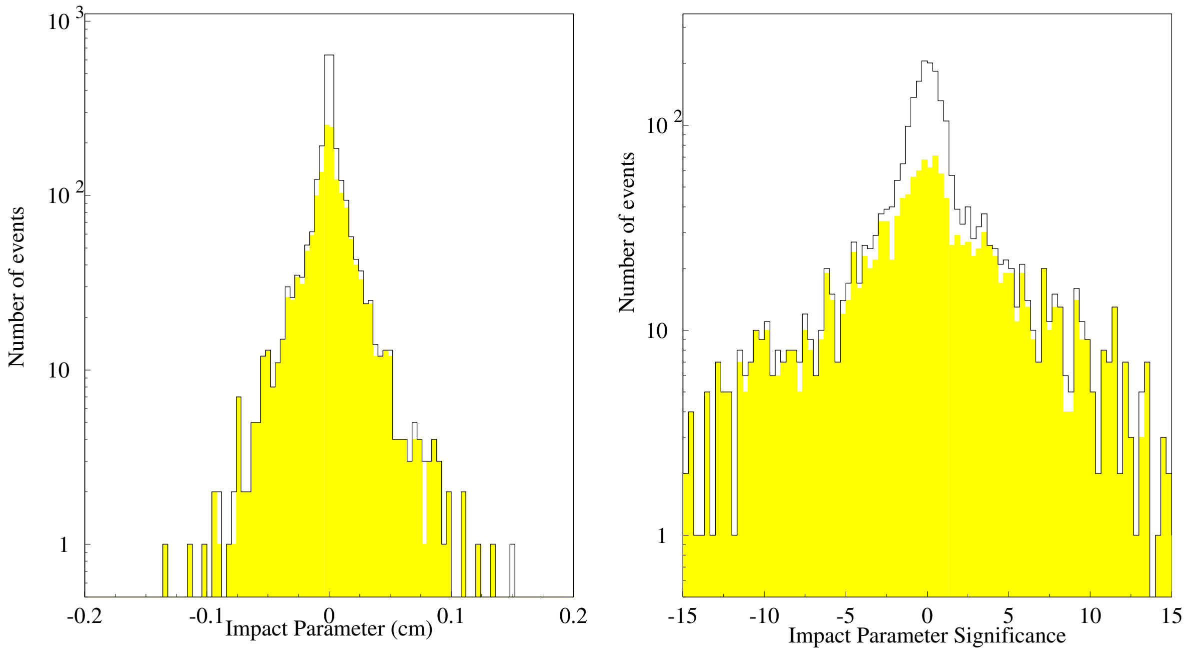

Figure 9: $Z \rightarrow b\bar{b}$: Impact parameter (left) and impact parameter significance (right) distribution of all tracks fitted by the Silicon Track Trigger. The shaded region corresponds to b-quark descendant tracks in the event.

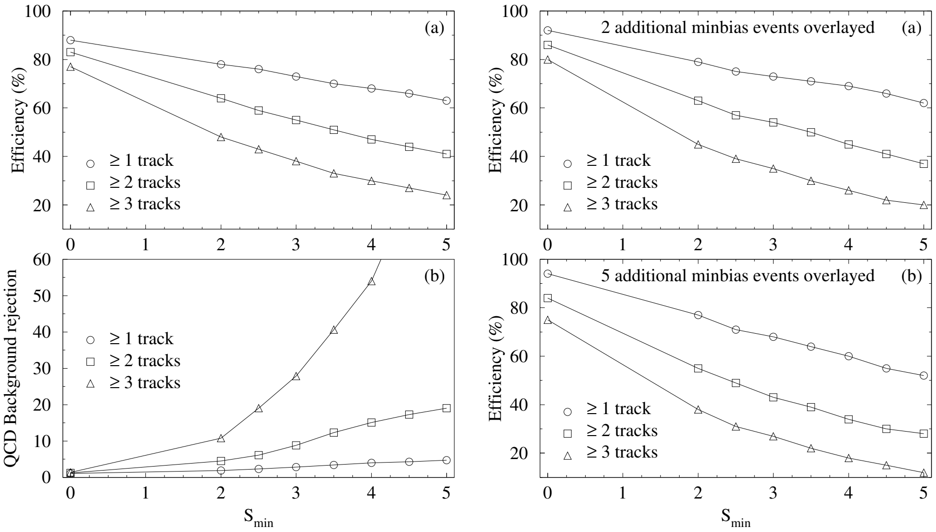

Figure 10: $Z \rightarrow b\bar{b}$: Efficiency and background rejection for various minimum STT track multiplicities as a function of the impact parameter significance threshold S_{min}. Efficiencies and background rejections are relative to the JET_2_MED trigger term; left: $Z \rightarrow b\bar{b}$ without additional interactions; right: with additonal minbias interactions.

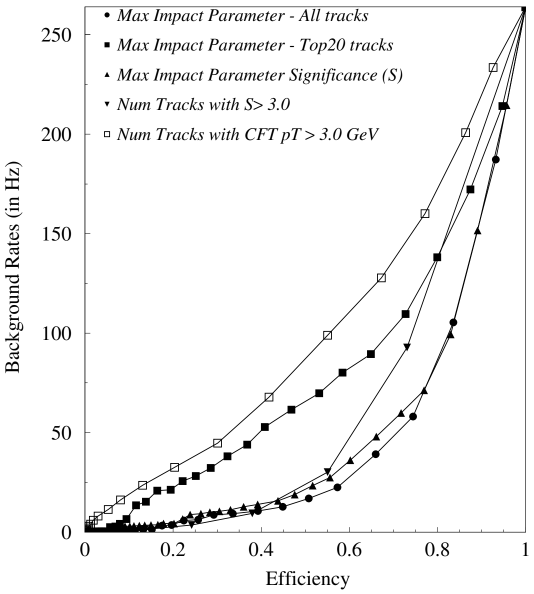

Figure 11: $Z \rightarrow b\bar{b}$: Efficiency vs. background rates for various trigger configurations using tracking information in additon to the JET_2_MED trigger. The efficiencies are computed relative to the JET_2_MED term.

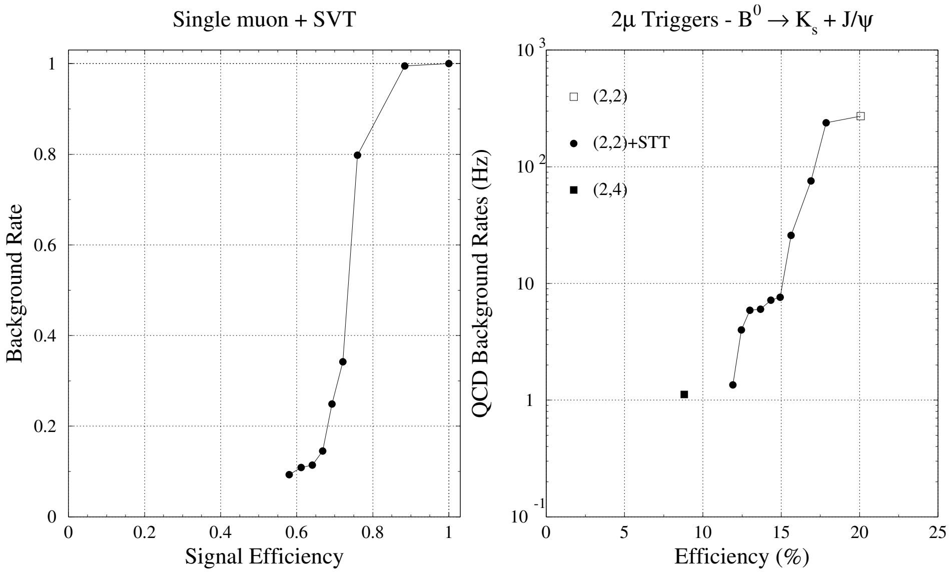

Figure 12: Background rate vs signal efficiency for (a) (left): $Q\bar{Q}$ events using a single muon trigger with STT, and (b) (right) for $B \rightarrow K_s + J/\psi$ events using a dimuon trigger, with and without STT, and with various p_t thresholds as indicated.

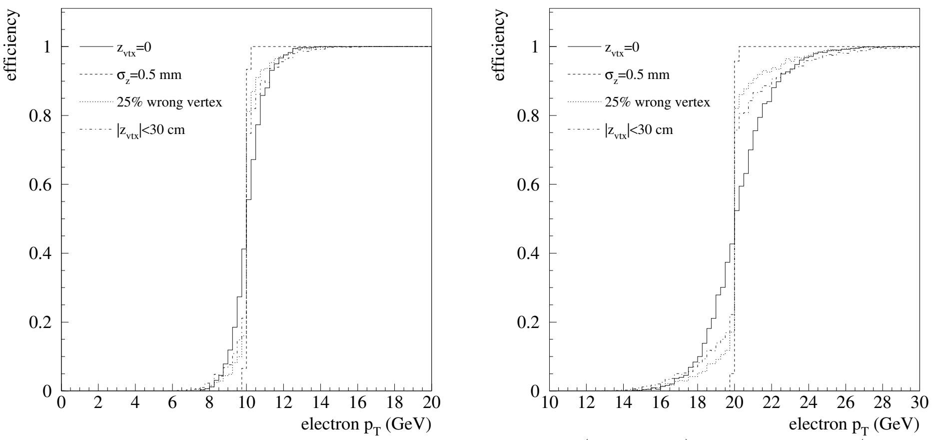

Figure 13: Turn-on curves for electrons with $E_T = 10$ GeV (left plot) and 20 GeV (right plot). The solid curve is with z-vertex assumed to be $= 0$, the dashed curve is with a reconstructed z-vertex with 100% reconstruction efficiency; the dotted curve takes into account the z-vertex reconstruction efficiency (78%), and the dash-dotted curve in addition accounts for the limited detector acceptance. The electron energy resolution is assumed to be $13\%/\sqrt{E}$, and the z_V resolution is taken to be 600μm.